

**A Methyl 4-Oxo-4-phenylbut-2-enoate with *in Vivo* Activity against MRSA that Inhibits
MenB in the Bacterial Menaquinone Biosynthesis Pathway**

Joe S. Matarlo[†], Yang Lu[†], Fereidoon Daryae[†], Taraneh Daryae[†], Bela Ruzsicska[†], Stephen G.
Walker[#] and Peter J. Tonge^{*,†}

Institute of Chemical Biology & Drug Discovery, [†]Department of Chemistry and [#]Department of
Oral Biology and Pathology, Stony Brook University, Stony Brook, NY, 11794-3400

Table S1: Comparison of theoretical vs observed ion isotopic distribution of **8**.

Table S2: Thermodynamic constants for the binding of CoA and CoA adducts **7** and **8** to *sa*MenB.

Figure S1: Role of Menaquinone (MK) in the Electron Transport Chain.

Figure S2: 4-Oxo-4-phenylbutanoic acids are able to mimic the transition state of the MenB
reaction by forming CoA adducts through a Michael addition reaction.

Figure S3: Menaquinone quantification in MRSA treated with ½ MIC of anti-bacterial agents.

Figure S4: Isothermal titration calorimetry (ITC) binding thermographs.

Figure S5: High Resolution LC/UV/MS ESI⁻ of OSB-CoA.

Figure S6: LC/ESI⁺ chromatograms for DHNA standard.

Figure S7: NMR and mass spectrum of compound **8**.

Table S1: Comparison of theoretical vs observed ion isotopic distribution of **8**. Molecular formula: C₃₂H₄₅ClN₇O₁₉P₃S. [M-H]⁻ m/z = 990.1315 and [M-2H]⁻² m/z = 494.5608.

| Theoretical | | Observed | | |
|-------------|---------------|----------|-----------|---------------|
| m/z | Abundance (%) | m/z | Abundance | Abundance (%) |
| 990.1320 | 100 | 990.1315 | 1014.79 | 100.00% |
| 991.1349 | 39.19 | 991.1335 | 347.95 | 34.29% |
| 992.1308 | 47.86 | 992.1301 | 392.43 | 38.67% |
| 993.1329 | 16.71 | 993.1325 | 37.73 | 3.72% |
| 994.1325 | 6.03 | | | |
| | | | | |
| Theoretical | | Observed | | |
| m/z | Abundance (%) | m/z | Abundance | Abundance (%) |
| 494.5623 | 100 | 494.5609 | 2451.61 | 100.00% |
| 495.0638 | 39.18 | 495.0630 | 1003.83 | 40.95% |
| 495.5618 | 47.85 | 495.5604 | 1145.04 | 46.71% |
| 496.0628 | 16.71 | 496.0626 | 386.26 | 15.76% |
| 496.5626 | 6.03 | 496.5613 | 28.86 | 1.18% |

Table S2: Thermodynamic constants for the binding of CoA
and CoA adducts **7** and **8** to *saMenB*

| | CoA | 7 | 8 |
|------------------------------|------------|----------|----------|
| K_d (μM) | 25.4 | 2.8 | 2.8 |
| ΔH^{\dagger} | -12.9 | -25.6 | -2.55 |
| $T\Delta S^{\dagger}$ | -6.7 | -18.1 | 4.93 |
| ΔG^{\dagger} | -6.2 | -7.5 | -7.5 |
| $\Delta\Delta G^{\dagger a}$ | | 1.3 | 1.3 |
| H-bond ^b | | +1 | +1 |

¹kcal/mol. ^aRelative to **CoA** ΔG . ^bPredicted hydrogen bond formed relative to CoA binding where 1 H bond = 1.4 kcal/mol.

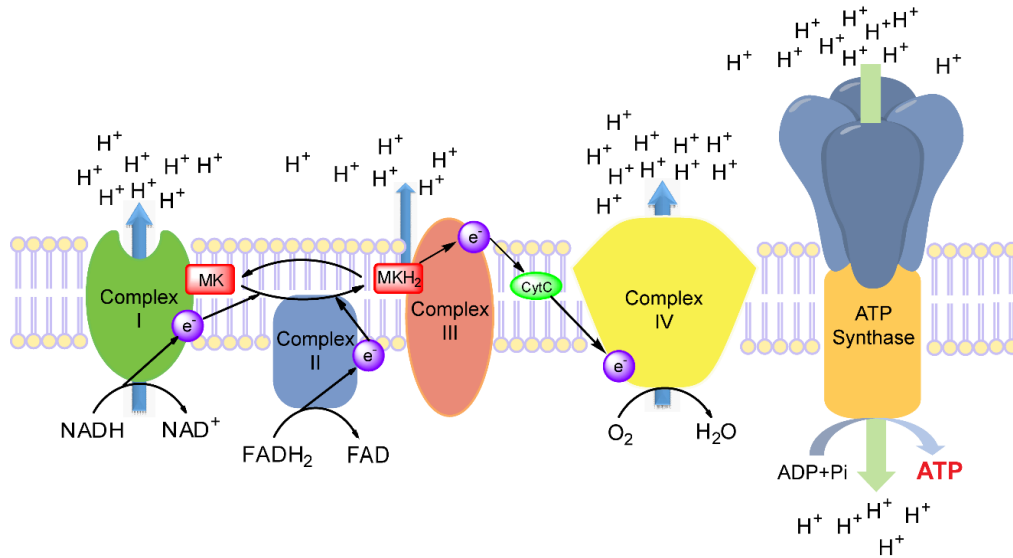


Figure S1: Role of Menaquinone (MK) in the Electron Transport Chain. MK (vitamin K2) is a lipid soluble redox active cofactor that shuttles reducing equivalents between components of the electron transport chain in human pathogens such as *S. aureus*. In *S. aureus*, MK functions as an electron carrier during both oxidative and fermentative respiration.

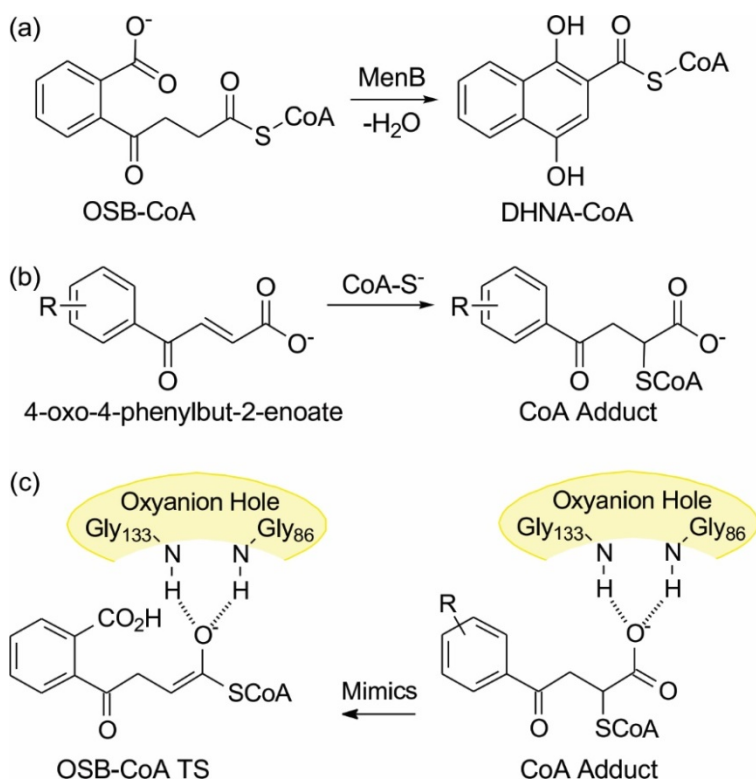


Figure S2: 4-Oxo-4-phenylbutanoic acids are able to mimic the transition state of the MenB reaction by forming CoA adducts through a Michael addition reaction. (a) MenB (1,4-dihydroxynaphthoyl-CoA synthase) catalyzes an intramolecular Dieckmann condensation leading to the formation of 1,4-dihydroxynaphthoyl-CoA (DHNA-CoA) from o-succinyl-benzoyl-CoA (OSB-CoA). (b) 4-oxo-4-phenylbut-2-enoates react with CoA to form adducts. (c) Adducts are transition state (TS) analogs of the MenB reaction in which the carboxylate binds in the MenB oxyanion hole (*E. coli* MenB numbering). This figure also shows the general structure of CoA adduct 7.^[46]

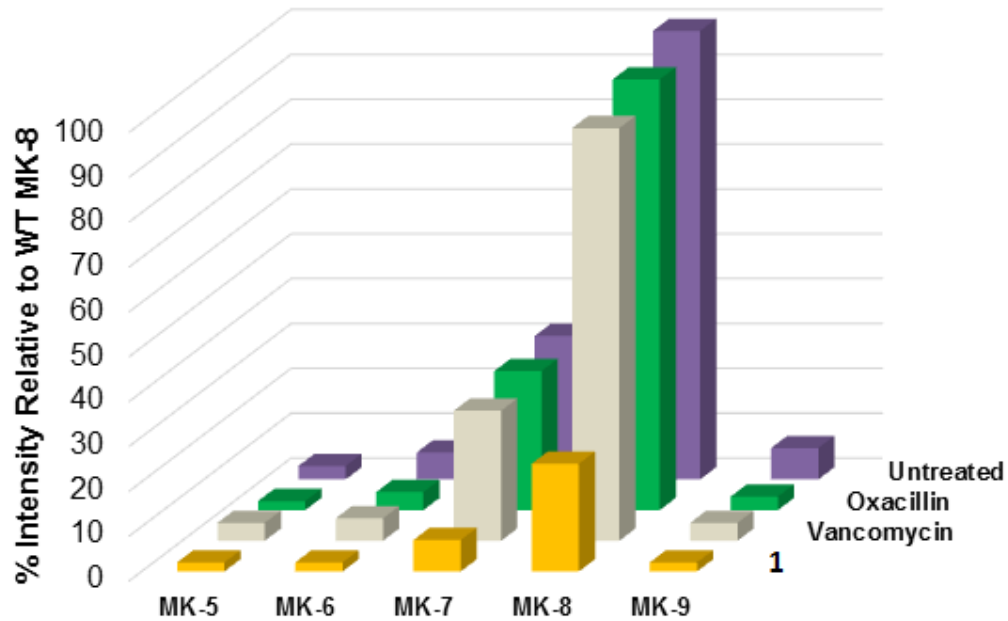


Figure S3: Menaquinone quantification in MRSA with or without anti-bacterial agents: 0.38 $\mu\text{g/mL}$ of **1**, 2 $\mu\text{g/mL}$ vancomycin, and 100 $\mu\text{g/mL}$ oxacillin. 10^9 cells per sample were analyzed for their change in MK levels. Each MK species is presented as a percentage (y-axis) where MK-8 = 100% in untreated MRSA. Vancomycin and oxacillin were also evaluated to determine if MK levels change upon treatment with these drugs.

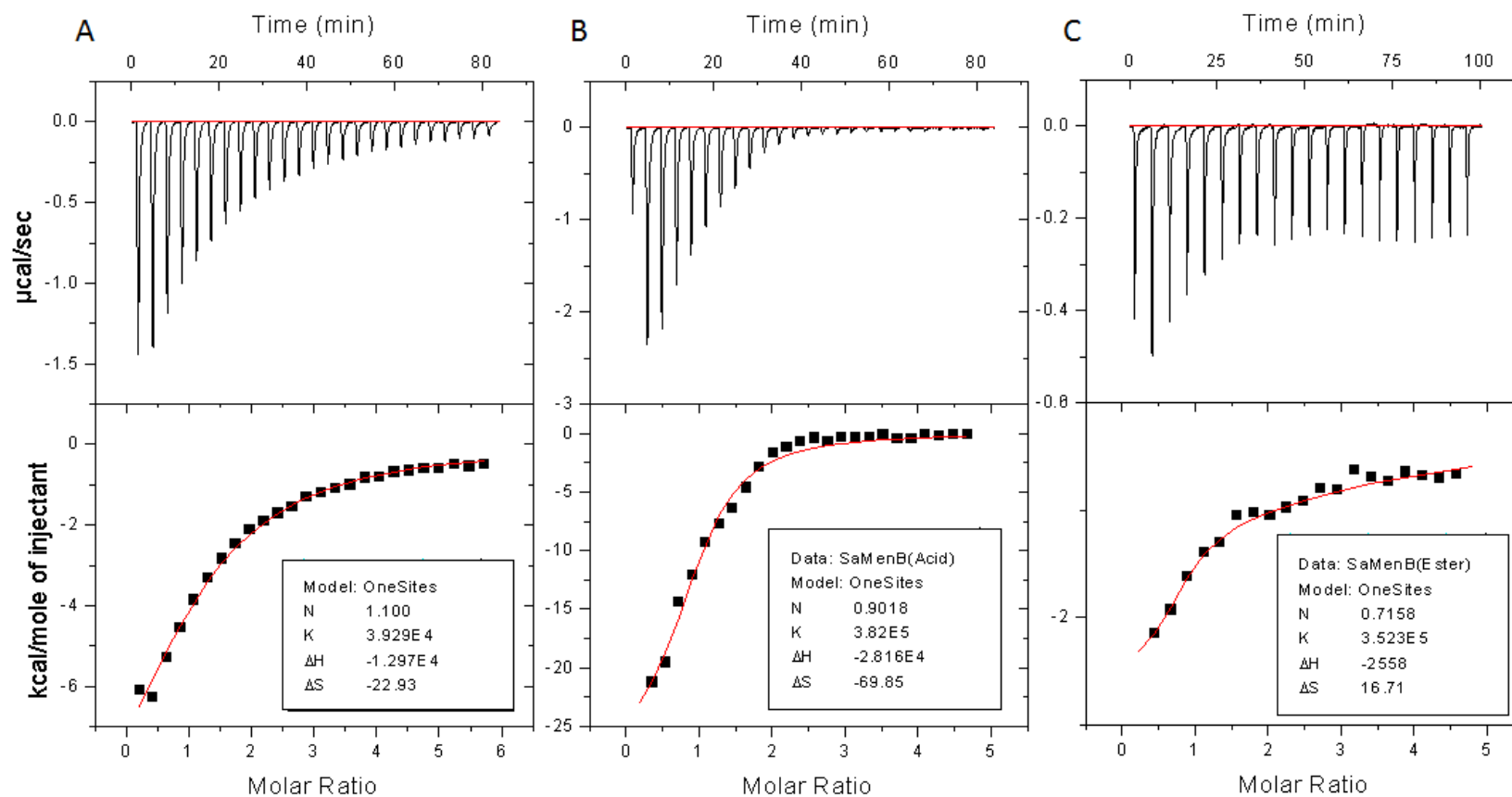


Figure S4: Isothermal titration calorimetry (ITC) binding thermographs. *saMenB* was titrated with (A) CoA, (B) **7**, and (C) **8** at 22 °C. Data were analyzed using a 1-site binding model. Ligands were prepared as a stock solution (2 mM) in the same buffer as that used for the protein (20 mM sodium phosphate pH 8.5, 250 mM NaCl, and 1 mM MgCl₂). In each case 4-8 µL aliquots of ligand were titrated into the ITC cell containing 1.8 mL of 25-50 µM purified *saMenB*. The titration period was 8-16 s with 300 s between each titration.

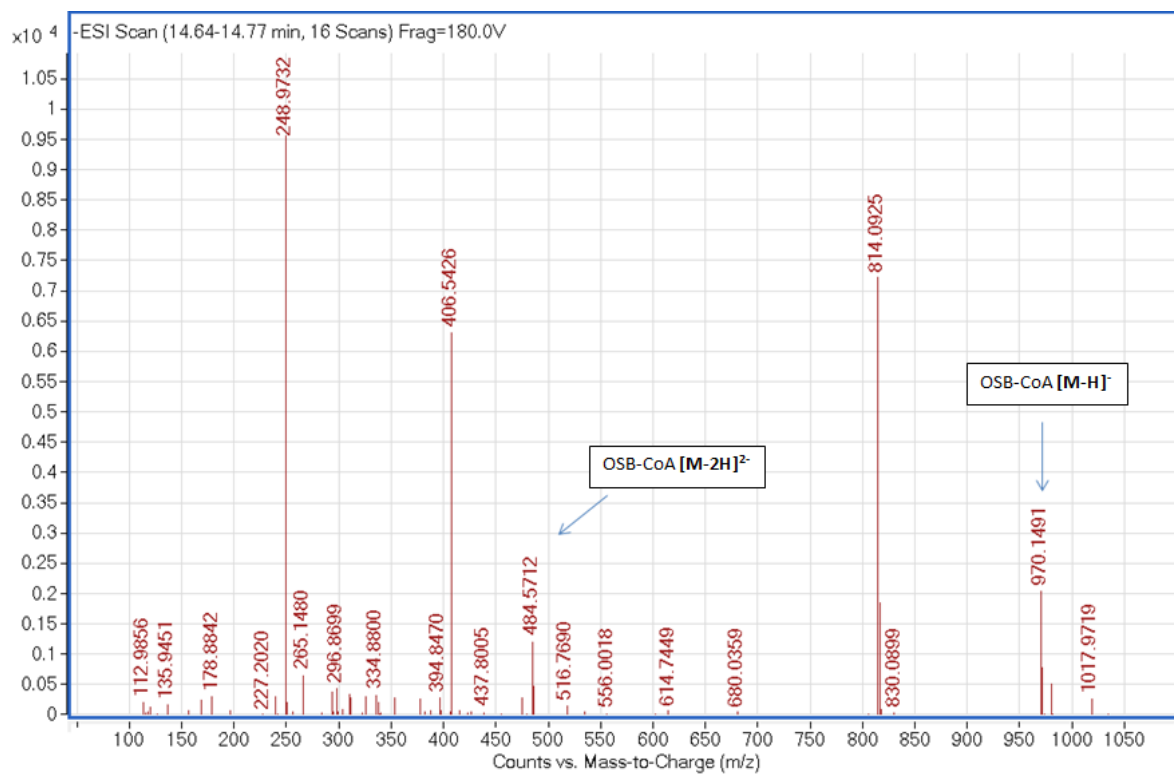


Figure S5: High Resolution LC/UV/MS ESI⁻ of OSB-CoA. OSB-CoA $m/z = 971.1491$ was enzymatically made by incubating MenE with OSB, ATP, and CoA for 1hour and filtering the product out. Observed peaks correspond to OSB-CoA EIC: [M-2H]²⁻ $m/z = 494.5711$, [M-H]⁻ $m/z = 970.1490$, 971.1525 . Extracts from **1** treated MRSA did not show accumulation of OSB-CoA.

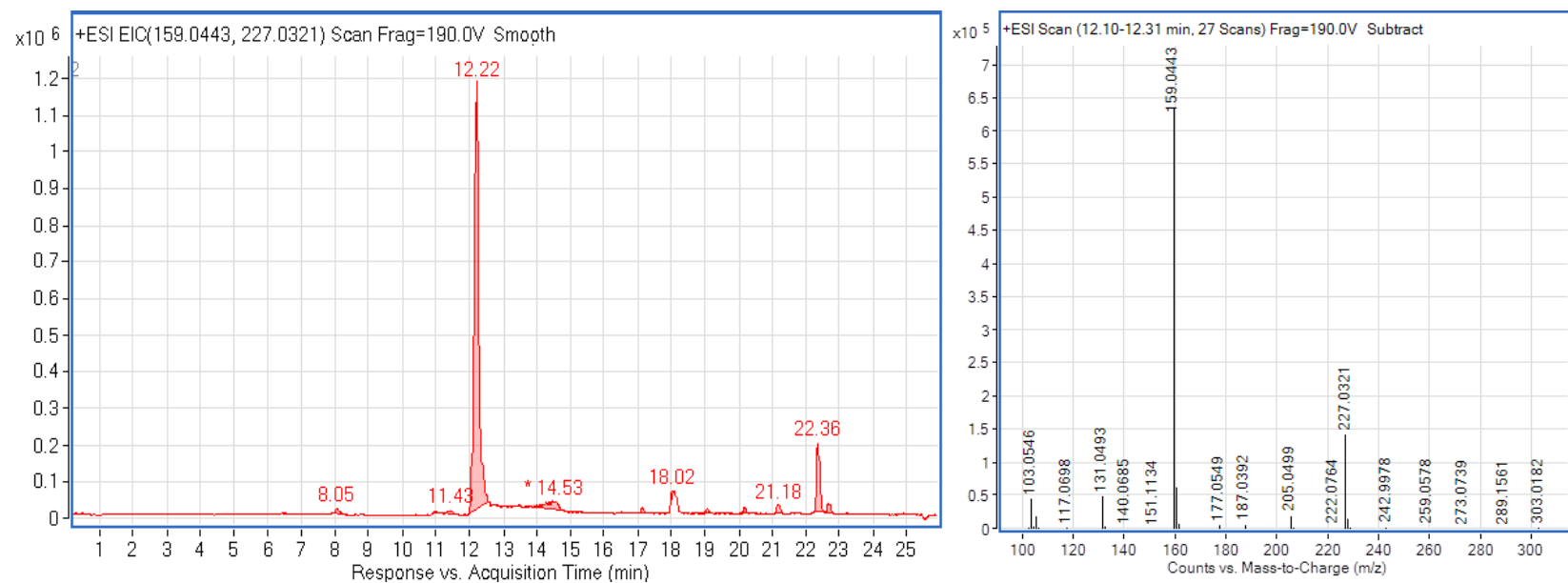


Figure S6: LC/ESI⁺ chromatograms for DHNA standard. The extracted mass spectra from the peak with retention time of 12.22 min shows that DHNA undergoes facile MS fragmentation with the loss of CO₂ to give a m/z =159.0442 ion. Other indicative ions are m/z = 227.0321, [M+Na]⁺ and fragment ions, m/z=131.0493 (CO loss) and 103.0546 (CO loss). The extracted UV spectra show an UV max of 275nm.

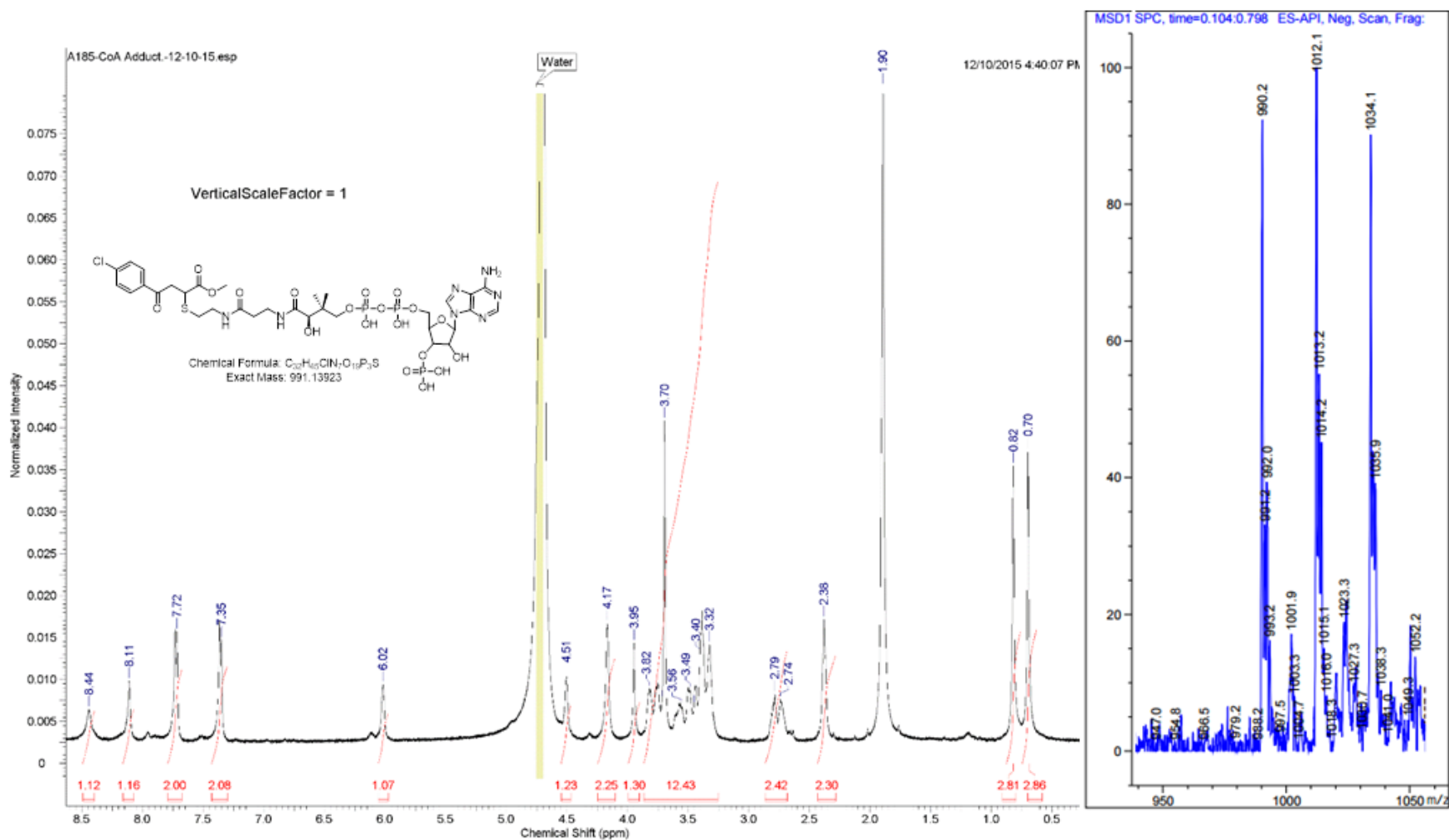


Figure S7: NMR (left) and MS ESI⁻ (right) of compound **8**. ¹H NMR (500 MHz, D₂O) δ ppm 0.70 (br. s., 3 H) 0.82 (br. s., 3 H) 2.38 (br. s., 2 H) 2.74 (br. s., 1 H) 2.79 (br. s., 1 H) 3.32 (br. s., 2 H) 3.36 - 3.52 (m, 4 H) 3.56 (br. s., 2 H) 3.63 - 3.77 (m, 4 H) 3.82 (br. s., 2 H) 3.95 (br. s., 1 H) 4.17 (br. s., 2 H) 4.51 (br. s., 1 H) 6.02 (br. s., 1 H) 7.36 (d, *J*=7.63 Hz, 2 H) 7.72 (d, *J*=7.93 Hz, 2 H) 8.11 (br. s., 1 H) 8.44 (br. s., 1 H). ESI⁻ calculated for [M-H]⁻ C₃₂H₄₅ClN₇O₁₉P₃S (compound **8**) is 990.13 observed 990.2.